ARTICLE

Pulse Electroplating of Nanotwinned Copper Using MPS-PEG Two-additive System for Damascene via Filling Process

Yu-Xi Wang [a,b], Li-Yin Gao [a,*], Yong-Qiang Wan [a], Zhe Li [a], Zhi-Quan Liu [a,b,*]

[a] Shenzhen Institute of Advanced Electronic Materials, Shenzhen Institute of Advanced Technology, Chinese Academy of Sciences, Shenzhen 518055, China
[b] Nano Science and Technology Institute, University of Science and Technology of China, Suzhou 215213, China

Abstract

High density nanotwinned copper films were pulse electroplated using an optimized electrolyte. In order to find out the influencing factors on the formation of nanotwins, series contents of MPS were added to the electrolyte during the pulse electroplating process. It was found that the copper films electroplated without MPS had large grains but a few nanotwins. And the grain size was about 0.9 μm on average, and the texture components of (110) and (111) crystal orientations were calculated as 49% and 27.8%, respectively. Differently, when 10 ppm MPS was added, the microstructure was changed to columnar grain with high density of horizontal nanotwins and the crystal orientation was also changed to highly (111) orientated one. However, when the MPS content was continuously increased from 10 ppm to 40 ppm, the microstructure and crystal orientation were almost unchanged as detected by the secondary ion microscopy of focus ion beam and X ray diffraction. Specifically, when 40 ppm MPS was used, the average grain size was 0.6 μm, and the texture components of (110) and (111) crystal orientations were 3.45% and 95.1%, respectively. It demonstrated that the nanotwinned copper can be electroplated at a large concentration range of MPS, which also meant that the filling ability of nanotwinned copper electrolyte could be adjusted by MPS content without influencing the microstructure. Finally, these electrolytes with different contents of MPS were used in the Damascene via filling. The results showed that when the content of MPS was 40 ppm, the Damascus via was completely filled without voids. The achievement of via filling with nanotwinned copper makes the application of nanotwinned copper possible in Integrated Circuit (IC) fabrication, which also greatly promotes the development of interconnected material for next generation.

Keywords: Pulse electroplating; Nanotwinned copper; via filling; Damascene process

1. Introduction

Due to its strong electromigration resistance, copper has been widely used as interconnection material in advanced packaging and Integrated Circuit (IC) fabrication. However, the miniaturization of line width and pitch put a great challenge on the properties and performance of traditional copper interconnected material [1–4]. Nanotwinned copper has exhibited ultra-high strength and excellent conductivity since its invention in 2004 [5]. Also, due to its excellent thermal stability and anti-oxidation performance [6], nanotwinned copper has also been regarded as a promising interconnected material in next generation [7,8]. Methods including direct current (DC) electroplating and pulse current (PC) electroplating of nanotwinned copper have been widely reported [9–11]. For example, Zhu et al. [12] filled the micro blind holes seamlessly with nanotwinned copper using gelatin as a single additive. Zhan et al. [13] had electroplated a highly (111) oriented

Received 23 September 2022; Received in revised form 23 November 2022; Accepted 2 December 2022
Available online 8 December 2022

* Corresponding author, Li-Yin Gao, Tel: (86-755)6665885, E-mail address: ly.gao@siat.ac.cn.
* Corresponding author, Zhi-Quan Liu, Tel: (86-755)86392104, E-mail address: zqliu@siat.ac.cn.

https://doi.org/10.13208/j.electrochem.2209231
1006-3471/© 2023 Xiamen University and Chinese Chemical Society. This is an open access article under the CC BY-NC license (http://creativecommons.org/licenses/by-nc/4.0/).

nanotwinned copper with a low Cu^{2+} concentration electrolyte without an additive by changing pulse frequency, which assisted the understanding of nanotwin formation. However, common additives, like MPS, JGB and PEG, are seldom used in most of nanotwinned copper electrolytes in literature [14]. The influence of additive content on via filling performance of nanotwinned copper during a pulse electroplated process remains uncertain [15].

Literature on copper via filling can also give insights [16−19]. Chen et al. [20] found that the ultrasonic power and pulse reverse current were beneficial to fill blind vias. Tao et al. [21] studied the synergistic effect of nitrogen-containing heterocyclic compound and other additives, and achieved void-free filling with outstanding uniformity. In order to achieve the applications in IC fabrication and advanced packaging, the filling capacity of nanotwinned electrolyte is further needed to be improved. However, it is difficult to simultaneously obtain the formation of high density nanotwinned microstructure and high filling capacity. According to our previous research, the addition of additives, like JGB, would interrupt the formation of nanotwins [22], which further led to the refinement of columnar grain and the decrease of nanotwin density with the increased JGB concentration.

In this study, the high density nanotwinned microstructure was obtained using an optimized electrolyte during a pulse electroplating. Series concentrations of accelerator, such as MPS, were added into the electrolyte in order to reveal the evolution of surface tomography, microstructure, texture and filling performance. The filling capacity of these nanotwinned copper films was also investigated in this study. The results showed that the Damascene via can be filled without voids at an appropriate MPS concentration. The achievement of via filling with the pulse electroplated nanotwinned copper broadens the application of nanowtinned copper films, and promotes the development of interconnected material for next generation.

2. Experimental

2.1. Material preparation

Nanotwinned copper was prepared by a pulse electroplating. A sourcemeter (Model 2461, Keithley) served as a pulse power supply. The anode was a Cu-P alloy, which contained about 0.05 wt% P. The cathode was silicon wafer coupon with or without via patterns. Before electroplating, a thin Cu seed layer was sputtered on the cathodic wafer coupon. The electroplating bath contained $CuSO_4\cdot 5H_2O$, H_2SO_4, Cl^-, MPS and PEG. The content of $CuSO_4\cdot 5H_2O$ was 50−100 $g\cdot L^{-1}$, the content of H_2SO_4 (98%) was 100−150 $mL\cdot L^{-1}$, and the concentration of Cl^- was about 50 ppm. The content of PEG was kept constant, while that of MPS was changing from 0 ppm to 40 ppm. Notably, being different from the direct current nanotwinned electrolyte reported in literature [23,24], no gelatin was added to our electrolyte. Nanotwins were generated by the stress induced by cyclic on-off pulses. The pulse on time was set at 20 ms, and the off time was set at 0.5−4 s, and the peak current density was set at 60 ASD. The rotation speed was set at 300 rpm, and the temperature was controlled at 25 ± 1 °C. Detailed information about the plating parameter and electrolyte bath has been reported previously [25]. Before electroplating, the cathodic substrate surface was cleaned with 5% dilute sulfuric acid and deionized water successively to remove the oxide [22].

2.2. Testing and characterization

The copper films electroplated with different contents of MPS were observed by focused ion beam (FIB, FEI, Helios 5UX) using the mode of secondary ion microscope (SIM). The voltage of 30 kV and current of 41 pA were used to observe the surface and the cross-section morphologies of the samples. Notably, for the cross-sectional examination, the cross section of the sample was firstly cut by ion beam before each observation. Moreover, the preferred crystal orientation of the sample was tested using X-ray diffraction (XRD, Bruker D8 Advance). The electron back-scattered diffraction (EBSD) test was also conducted to observe the microstructural characteristic of electroplated copper films. Before each EBSD observation, the samples were ground with 5000 # abrasive paper and polished with Al_2O_3 paste mechanically. Then an ion milling was conducted on the top view of films to remove the deformation layer from the samples. The working voltage and current were 5 kV and 45−50 μA, respectively, for 15 min in the first step, 3 kV and 18−25 μA, respectively, for 20min in the second step, and then 1.5 kV and 10−15 μA, respectively, for 30 min in the third step.

3. Results and discussion

3.1. Surface morphology of electroplating copper films

Fig. 1 shows the surface morphologies of the pulse electroplated copper film samples with the concentrations of MPS varying from 0 ppm to

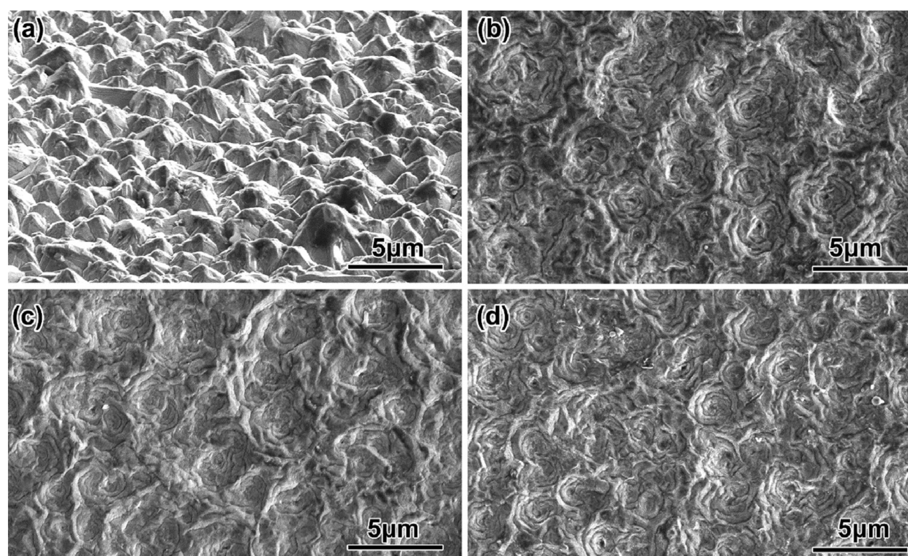

Fig. 1. The top view SEM images of pulse electroplated copper films with different MPS concentrations: (a) 0 ppm, (b) 10 ppm, (c) 20 ppm and (d) 40 ppm.

40 ppm. As shown in Fig. 1a, the surface roughness of the sample without MPS was the largest, which consisted of copper cones. While 10 ppm MPS was added (Fig. 1b), the sample surface was relatively smooth, where many circular steps can be observed. It seems that the circular step was inducted by nanotwins [26,27]. With the increase of MPS content, no significant changes were detected from the surface morphology (20 ppm in Figs. 1c and 40 ppm in Fig. 1d). The surface roughness (*S*a) of different samples was confirmed by laser confocal microscopy (LSCM) quantitatively. More than three locations (area of 100 μm × 100 μm) were measured in order to obtain the average value. As a result, the *S*a values for the samples deposited with 0, 10, 20 and 40 ppm MPS were estimated to be 660 nm, 333 nm, 316 nm and 330 nm, respectively.

Therefore, it is concluded that the addition of MPS can change the surface morphology obviously, but the successively increasing of MPS content has little impact on the surface morphology.

3.2. Cross-sectional microstructure of electroplating copper films

The cross-sectional microstructure of pulse electroplated films with different MPS contents is shown in Fig. 2. As revealed in Fig. 2a, large grains were detected when no MPS was added. The large grain corresponds to a cone on the surface, which is consistent with the description in Fig. 1a. And there were some nanotwinned boundaries within the large grains. The direction of nanotwinned boundary was basically anisotropic. When 10 ppm was added (Fig. 2b), some fine grains were detected at the interface between seed layer and columnar grains. Upon the fine grains, columnar grains with high density of nanotwinned boundary were detected. Notably, the nanotwinned boundary was basically in a horizontal direction, which was perpendicular to the growth direction of copper films. When the MPS content was increased to 20 ppm, no obvious change in the microstructure of copper film was observed. When the MPS was further increased to 40 ppm, similar microstructure was observed. However, the twin lamella seemed to be enlarged slightly. The result also demonstrated that the microstructure was changed when the MPS was added, while kept stable when the MPS content was increased.

3.3. Crystal structure of electroplating copper films

As shown in Fig. 3a, XRD spectra of different copper films are presented. The films without MPS had two obvious peaks as denoted by (111) and (220) according to the JCPDS card. The texture coefficient (TC) values are calculated using the following equation [28]:

$$TC_{(hkl)} = \frac{I_{(hkl)}/I_{0(hkl)}}{(1/n)\sum I_{(hkl)}/I_{0(hkl)}} \quad (1)$$

where $I_{(hkl)}$ is the peak intensity of the (hkl) diffraction plane, $I_{0(hkl)}$ is the standard peak intensity of (hkl) diffraction plane in the JCPDS card, and n is the number of diffraction peaks, and $n = 3$ here. The results of TC are given in Fig. 3b. The TC value of (111) was 1.61, while (220) was 1.35, which

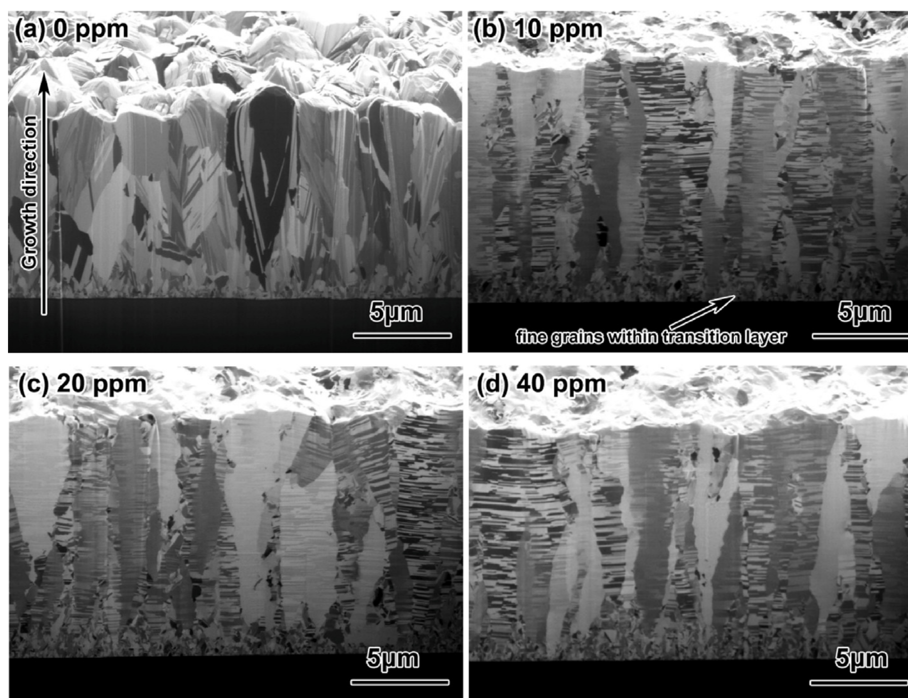

Fig. 2. The cross-sectional microstructure of pulse electroplated copper films with different MPS concentrations: (a) 0 ppm, (b) 10 ppm, (c) 20 ppm and (d) 40 ppm.

means that both the intensities of (111) and (220) diffraction planes are strong. When 10−40 ppm MPS were added, only a strong (111) peak was detected from the XRD spectra in Fig. 3a. The TC value of (111) diffraction plane increased to 2.97−2.98 as given in Fig. 3b, indicating a very strong (111) preferred orientation.

EBSD characterization was also performed on the pulse electroplated copper films. The band contrast image of copper films electroplated with 0 ppm MPS is given in Fig. 4a. The small angle grain boundaries, the large angle grain boundaries and the Sigma 3 (111) nanotwinned boundaries are illustrated in grey, black and red, respectively. The average grain size was calculated as 0.9 μm using Channel 5 software. Also, the length proportion of grain boundaries and twin boundaries were calculated, and the results are given in the upper right inset. The length proportion of twin boundaries for the 0 ppm MPS sample was about 70.5%. The corresponding Inverse Pole Figure (IPF) results in Z direction are also displayed in Fig. 4b. Both the (111) and (110) textures were detected, and the texture components of (110) and (111) orientations were about 49% and 27.8%, respectively. Notably, the crystal plane index (110) here is a Miller index, which represents the same orientation as the (220) diffraction plane during the XRD

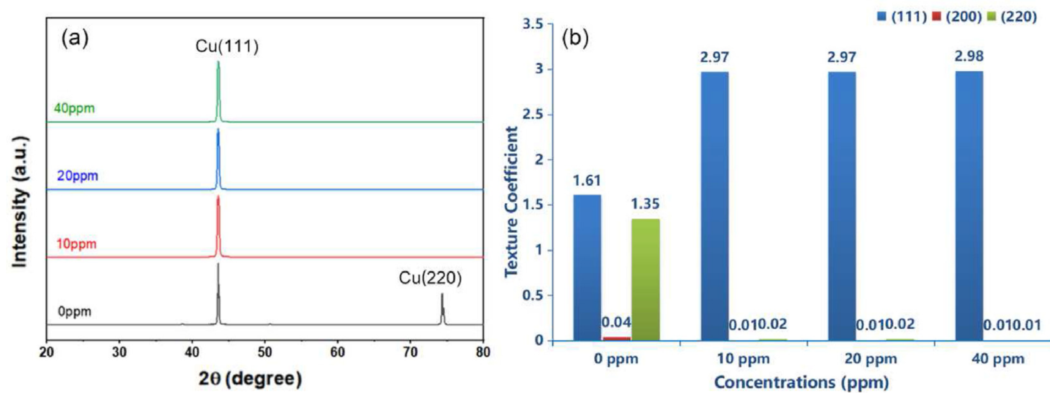

Fig. 3. (a) XRD spectra and (b) the corresponding texture coefficient calculations of pulse electroplated copper film with different MPS concentrations.

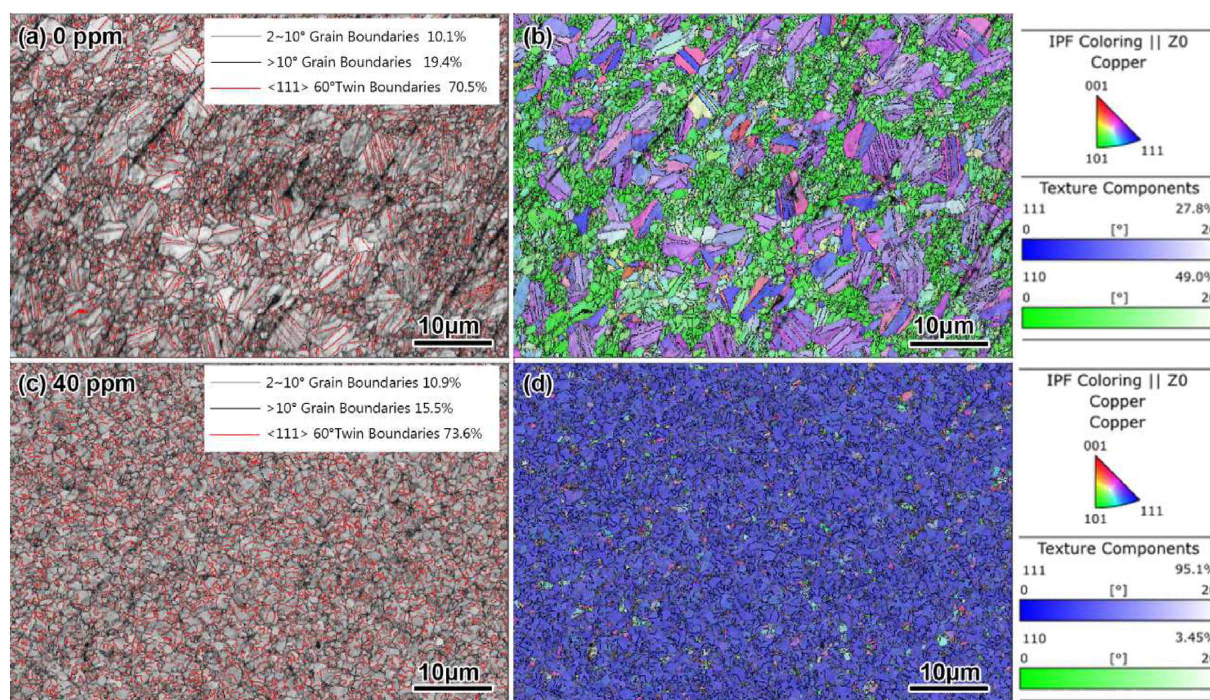

Fig. 4. The EBSD analysis of the pulse electroplated copper films with different MPS concentrations: (a) band contrast image and (b) IPF Z image with 0 ppm; (c) band contrast image and (d) IPF Z image with 40 ppm.

measurements. The situation of copper films electroplated with the 40 ppm MPS is given in Fig. 4c and d. The grain size was estimated as 0.6 μm, which was greatly decreased as compared to the status without MPS. Also, the length proportion of the twin boundaries was calculated as 73.6%, indicating an increase in the twin boundary of the 40 ppm MPS sample. The IPF Z map and calculated results are shown in Fig. 4d. And it is noticed that the image was almost in blue, representing a high proportion of (111) orientation. The texture component of (110) orientation was minimized to 3.45%, while that of (111) orientation was as high as 95.1%.

In order to reveal the effects of pulse current, and additions of PEG and MPS contents on the formation of nanotwins, comparative studies were conducted. Firstly, the samples were prepared by direct current electroplating instead of pulse current, while the other parameters were kept constant as in Fig. 2a and d. The current density used in the direct current density of electroplating was set as the average current density of pulse electroplating, following the below equation:

$$J_{av} = J_p * T_{on} / (T_{on} + T_{off}) \quad (2)$$

J_{av} is the average current density of the direct current electroplating, and J_p is the peak current density of the pulse current electroplating, and T_{on} is the time at the peak current, and T_{off} is the time without passing the current. The average direct current density can be calculated to be 0.6 $A \cdot dm^{-2}$. The microstructures of the samples prepared using a direct current density of 0.6 $A \cdot dm^{-2}$ with 0 and 40 ppm MPS are given in Fig. 5a−b. The nanotwin density was decreased dramatically when used direct current. It can be deduced that pulse current promotes the formation of nanotwins. As reported in literature that the on and off pulses produce cyclic stress, which further leads to the formation of nanotwins in order to minimize the total energy of system [29,30].

Secondly, in order to reveal the role of PEG addition, comparative studies without PEG were also conducted. Besides the absence of PEG, other parameters were kept constant as in Fig. 2a and d. As shown in the SIM images of Fig. 5c and d, the regularity of microstructure was decreased without PEG. For the 0 ppm MPS sample, the nanotwin was basically vertical and the texture was (110) with PEG (Fig. 2a). And the direction of nanotwin was random and the texture was changed to (111) when the PEG was absent (Fig. 5c). For the 40 ppm MPS sample, the nanotwin was basically horizontal with PEG (Fig. 2d), while some inclined nanotwins appeared without PEG (Fig. 5d).

It can thus safely conclude that the addition of MPS promoted the formation of high density nanotwinned microstructure, while the addition

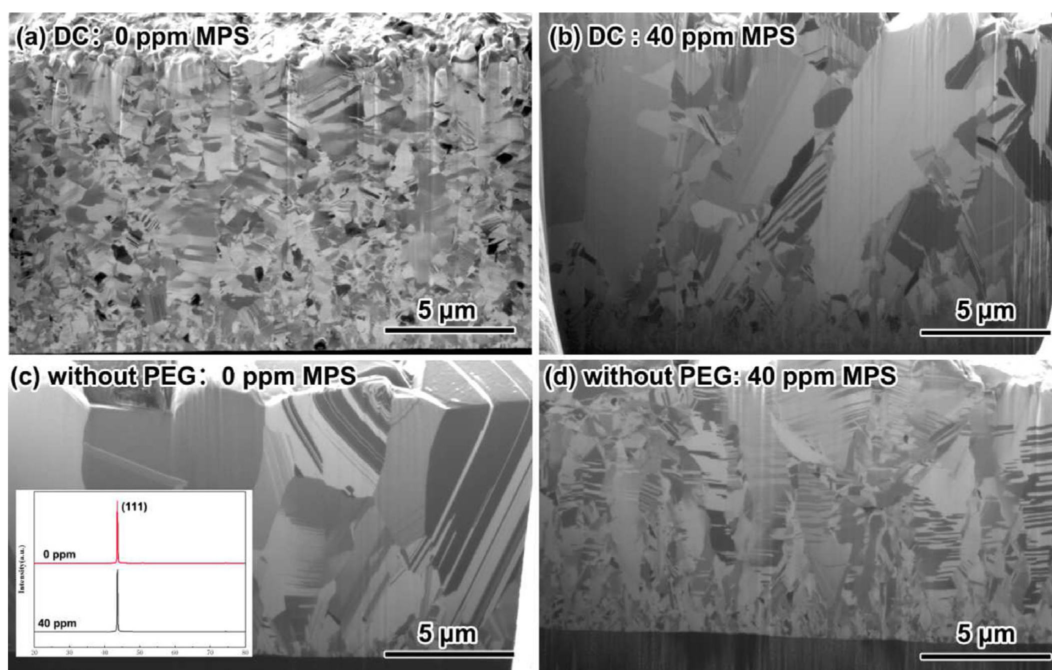

Fig. 5. Comparative studies: (a) the samples prepared by direct current electroplating with 0 ppm MPS and (b) 40 ppm MPS; (c) the samples prepared by pulse electroplating with 0 ppm MPS but without PEG and (d) with 40 ppm MPS but without PEG.

PEG improved the regularity of microstructure. Probably, the adsorption of MPS upon the copper surface would increase stress. So more twinned boundaries were generated when the additive MPS was used. On the other hand, MPS was served as an accelerator during copper electrodeposition, and it would decrease the crystallization overvoltage [31]. And it was reported that the decrease of crystallization overvoltage was beneficial for the nuclei and growth of (111) orientation [32]. The (111) orientated nanotwinned microstructure with a smaller grain size was then obtained after the addition of MPS. However, the intrinsic mechanism was still under investigation.

Above all, the microstructure was changed greatly after the addition of MPS. However, the typical microstructure of columnar grains with high density nanotwinned boundary was detected no matter how the MPS concentrations changed from 10 ppm to 40 ppm, showing little evolution. The achievement of electroplating high density nanotwinned copper at a wide range of MPS concentration means that their filling ability can be adjusted by varying MPS concentration without influencing the formation of nanotwins.

3.4. The filling performance of Damascene vias

Damascene vias were prepared to check the filling performance of electrolytes with different contents of MPS. The Damascene vias were trapezoidal (Fig. 6a). And as enlarged in Fig. 6b, a single via was about 1.4 μm deep, 1.4 μm wide at the bottom and 1.9 μm wide at the top. The aspect ratio was about 1:1.

The filling performance is given in Fig. 7. When the electrolyte was free of MPS, the microstructure consisted of large grains, and few nanotwinned boundaries were detected. And it was noticed that there was a small void at the center of via (Fig. 7a'), which means that the solo additive PEG could not fill the via seamlessly. When 10 ppm and 20 ppm MPS were added, the microstructure consisted of columnar grains and nanotwinned boundaries (Fig. 7b and c) could be observed. The microstructure in Fig. 7 far from via is consistent with that in Fig. 1. However, it was noticed that the regularities of columnar grains and horizontal nanotwins were interrupted at the top and bottom of via since the current distribution of via was not uniform. The grains would be refined within the via, and most of nanotwins boundaries were inclined. Also, voids were detected as given in Fig. 7b' and c', demonstrating a poor filling capacity for the 10 ppm and 20 ppm MPS samples. When the MPS content was further increased to 40 ppm, the via was filled without voids as shown in Fig. 7d'. The increased content of accelerator promotes the copper deposition at the bottom of via, so the via was filled completely.

Notably, since the convection condition and current distribution for plane surface were different in Damascene via, the microstructure showed a small difference between plane surface (Fig. 2) and via filling (Fig. 7). However, the vertical

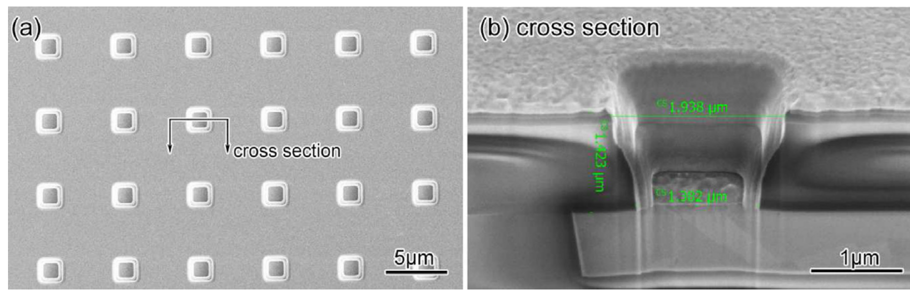

Fig. 6. (a) Damascene vias before electroplating; (b) and the enlarged cross-section of a single via.

and horizontal twinned structures were still observed during the Damascene via filling as highlighted in Fig. 6, which can match the deposition on plane surface. Also, the microstructures of the samples (Fig. 7b'−d') deposited with 10−40 ppm MPS showed little changes. In addition, the time for filling deposition was all controlled as 8080 s, and the thicknesses of the electrodeposits were about 1.5−1.7 μm as shown in Fig. 7. Hence, the growth rate was calculated as

Fig. 7. The filling performance of Damascene vias using different MPS concentrations: (a) 0 ppm, (b) 10 ppm, (c) 20 ppm and (d) 40 ppm; and the single vias are enlarged in (a'−d') correspondingly.

0.11−0.13 $\mu m \cdot min^{-1}$, which displayed a small difference when the MPS content was increased from 0 to 40 ppm.

Above all, the suitable concentration of MPS additive was obtained at 40 ppm. And the Damascene vias can be filled with nanotwinned copper using PEG-MPS two-additive system during pulse electroplating.

4. Conclusions

A two-additive copper electrolyte system, i.e., MPS-PEG, was investigated during pulse electroplated nanotwinned copper films. Upon electroplating without MPS, the film consisted of coarse grains with an average diameter of 0.9 μm. And there existed some vertical or inclined nanotwinned boundaries within the films. Also, the texture components of (110) and (111) within the films were estimated to be 49% and 27.8%, respectively. As inferred from the FIB observation and XRD analysis, when 10 ppm MPS was added, the surface morphology was changed from cone to circular steps, and the microstructure was transformed from large columnar grains with a few nanotwins into columnar grains with high density horizontal nanotwins, furthermore, the crystal orientation was also turned from anisotropic to highly (111) orientated one. But when the content of MPS was further increased from 10 ppm to 40 ppm, the surface morphology, microstructure and crystal texture showed little changes. It indicates that the nanotwinned microstructure was non-sensitive to the concentration of MPS, which provides the convenience of adjusting filling capacity by adding MPS. Specifically, the grain size was refined to 0.6 μm in diameter, and the texture components of (110) and (111) were 3.45% and 95.1%, respectively, with 40 ppm MPS. Moreover, for the 1.9 μm wide and 1.4 μm deep Damascene vias, the suitable MPS concentration of void-less filling was about 40 ppm. The higher content of MPS can promote the deposition at the bottom of via, which further eliminates the voids. The enhancement of filling capacity of nanotwinned electrolyte broadens the application of nanotwinned copper films.

Acknowledgements

This work was financially supported by the Guangdong Basic and Applied Basic Research Foundation (Grant No. 2022A1515011485), National Natural Science Foundation of China (Grant No. 62104243), SIAT Innovation Program for Excellent Young Researchers and Shenzhen Post-doctoral Funding.

References

[1] Cho D H, Seo S M, Kim J B, Rajendran S H, Jung J P. A review on the fabrication and reliability of three-dimensional integration technologies for microelectronic packaging: through-Si-Via and solder bumping process[J]. Metals, 2021, 11(10): 1664.

[2] Tu K N. Reliability challenges in 3D IC packaging technology[J]. Microelectron. Reliab., 2011, 51(3): 517−523.

[3] Shen Y, Li B B, Ma Y, Wang Z L. Research progress in electroless cobalt plating and the bottom-up filling of electroless plating[J]. J. Electrochem., 2022, 28(7): 2213002.

[4] Tan B Z, Liang J L, Lai Z L, Luo J Y. Electrochemical deposition of copper pillar bumps with high uniformity[J]. J. Electrochem., 2022, 28(7): 2213004.

[5] Lu L, Shen Y F, Chen X H, Qian L H, Lu K. Ultrahigh strength and high electrical conductivity in copper[J]. Science, 2004, 304(5669): 422−426.

[6] Tseng C H, Tu K N, Chen C. Comparison of oxidation in uni-directionally and randomly oriented cu films for low temperature Cu-to-Cu direct bonding[J]. Sci. Rep., 2018, 8(1): 1−7.

[7] Sun F L, Liu Z Q, Li C F, Zhu Q S, Zhang H, Suganuma K. Bottom-up electrodeposition of large-scale nanotwinned copper within 3D through silicon via[J]. Materials, 2018, 11(2): 319.

[8] Huang J, Gao L Y, Peng Z J, Li Z, Liu Z Q, Sun R. Effect of sodium thiazolinyl dithiopropane sulphonate (SH110) addition on electroplating nanotwinned copper films and their filling performance of fine-pitch redistributed layer (RDL)[J]. Nanotechnology, 2023, 34(1): 015710.

[9] Dong M Y, Chen P X, Hang T, Li M. Nanotwinned copper micro-cone array fabricated by pulse electrodeposition for low-temperature bonding - sciencedirect[J]. Materials Letters, 290: 129470.

[10] Bai Y, Hu H, Ling H Q, Hang T, Hu A M, Wu Y M, Li M. Communication—fabrication of vertical nanotwinned copper with (220) texture by direct current electrodeposition[J]. J. Electrochem. Soc., 2021, 168(8): 082506.

[11] Li Y J, Tu K N, Chen C. Tensile properties and thermal stability of unidirectionally< 111>-oriented nanotwinned and< 110>-oriented microtwinned copper[J]. Materials, 2020, 13(5): 1211.

[12] Zhu Q S, Zhang X, Li S J, Liu C Z, Li C F. Communication—electrodeposition of nano-twinned Cu in void-free filling for blind microvia of high density interconnect[J]. J. Electrochem. Soc., 2019, 166(1): D3097−D3099.

[13] Zhan X F, Lian J, Li H J, Wang X B, Zhou J A, Trieu K, Zhang X P. Preparation of highly (111) textured nanotwinned copper by medium-frequency pulsed electrodeposition in an additive-free electrolyte[J]. Electrochim. Acta, 2020, 365: 137391.

[14] Hai N TM, Huynh T TM, Fluegel A, Arnold M, Mayer D, Reckien W, Bredow T, Broekmann P. Competitive anion/anion interactions on copper surfaces relevant for damascene electroplating[J]. Electrochim. Acta, 2012, 70: 286−295.

[15] Zhang Y B, Gao L Y, Li X, Li Z, Ma X L, Liu Z Q, Sun R. Electroplating nanotwinned copper for ultrafine pitch redistribution Layer (RDL) of advanced packaging technology. 2021 22nd international conference on electronic packaging technology (ICEPT): IEEE, 2021: 1−6.

[16] Du L, Shi T L, Su L, Xue D M, Liao G L. A novel bottom-up copper filling of blind silicon vias in 3d electronic packaging[J]. J. Micromech. Microeng., 2015, 25(4): 045005.

[17] Zhou Z H, Tan C L, Xiong W, Xi D L, Liu B Y. Introduction of development and application technology of organic

additives for acid copper electroplating[J]. J. Electrochem., 2022, 28(6): 2104531.

[18] Meng Y C, Zhou M M, Huang W, Min Y L, Shen X X, Xu Q J. Benzyl-containing quaternary ammonium salt as a new leveler for microvia copper electroplating[J]. Electrochim. Acta, 2022, 429: 141013.

[19] Zhou M M, Meng Y C, Ling J W, Zhang Y, Huang W, Min Y L, Shen X X, Xu Q J. 5-Amino-1,3,4-Thiadiazole-2-Thiol as a new leveler for blind holes copper electroplating: theoretical calculation and electrochemical studies[J]. Appl. Surf. Sci., 2022, 606: 154871.

[20] Chen Q W, Wang Z Y, Cai J, Liu L T. The influence of ultrasonic agitation on copper electroplating of blind-vias for soi three-dimensional integration[J]. Microelectron. Eng., 2010, 87(3): 527−531.

[21] Tao Z H, Long Z Y, Tengxu L J, Liu G T, Tao X F. The synergistic effects of additives on the micro vias copper filling[J]. J. Electroanal. Chem. 2022: 116456.

[22] Huang J, Gao L Y, Liu Z Q. The electrochemical behavior of leveler JGB during electroplating of nanotwinned copper [C]//2020 21st International Conference on Electronic Packaging Technology (ICEPT): IEEE, 2020: 1−4.

[23] Sun F L, Gao L Y, Liu Z Q, Zhang H, Sugahara T, Nagao S, Suganuma K. Electrodeposition and growth mechanism of preferentially orientated nanotwinned Cu on silicon wafer substrate[J]. J. Mater. Sci. Technol., 2018, 34(10): 1885−1890.

[24] Li Z G, Gao L Y, Li Z, Sun R, Liu Z Q. Regulating the orientation and distribution of nanotwins by trace of gelatin during direct current electroplating copper on titanium substrate[J]. J. Mater. Sci., 2022, 57(37): 17797−17811.

[25] Wang Y X, Gao L Y, Wan Y Q, Liu Z Q, Sun R. Effect of pulse off time on microstructure and properties of twinned copper films by pulse electrodeposition[C]// 2022 23rd International conference on electronic packaging technology (ICEPT), Dalian, China, 2022: 1−5.

[26] Chan T C, Lin Y M, Tsai H W, Wang Z M, Liao C N, Chueh Y L. Growth of large-scale nanotwinned Cu nanowire arrays from anodic aluminum oxide membrane by electrochemical deposition process: controllable nanotwin density and growth orientation with enhanced electrical endurance performance [J]. Nanoscale, 2014, 6(13): 7332−7338.

[27] Hsiao H Y, Liu C M, Lin H W, Liu T C, Lu C L, Huang Y S, Chen C, Tu K N. Unidirectional growth of microbumps on (111)-oriented and nanotwinned copper[J]. Science, 2012, 336(6084): 1007−1010.

[28] Pavithra C LP, Sarada B V, Rajulapati K V, Ramakrishna M, Gundakaram R C, Rao T N, Sundararajan G. Controllable crystallographic texture in copper foils exhibiting enhanced mechanical and electrical properties by pulse reverse electrodeposition[J]. Cryst. Growth Des., 2015, 15(9): 4448−4458.

[29] Xu D, Kwan W L, Chen K, Zhang X, Ozolins V, Tu K N. Nanotwin formation in copper thin films by stress/strain relaxation in pulse electrodeposition[J]. Appl. Phys. Lett., 2007, 91(25): 254105.

[30] Marro J B, Darroudi T, Okoro C A, Obeng Y S, Richardson K C. The influence of pulse plating frequency and duty cycle on the microstructure and stress state of electroplated copper films [J]. Thin Solid Films, 2017, 621: 91−97.

[31] Wang C, Zhang J Q, Yang P X, An M Z. Through-hole filling by copper electroplating using sodium thiazolinyl-dithiopropane sulfonate as the single additive[J]. Int. J. Electrochem. Sci., 2012, 7(11): 10644−10651.

[32] Hong B, Jiang C H, Wang X J. Influence of complexing agents on texture formation of electrodeposited copper[J]. Surf. Coat Technol., 2007, 201(16−17): 7449−7452.

应用于大马士革工艺的纳米孪晶铜脉冲电沉积研究

王玉玺 [a,b]，高丽茵 [a,*]，万永强 [a]，李哲 [a]，刘志权 [a,b,*]
[a] 中国科学院深圳先进技术研究院，深圳先进电子材料国际创新研究院，广东 深圳 518055
[b] 中国科学技术大学纳米科学技术学院，江苏 苏州 215213

摘要

本文在前期优化的电镀液的基础上，使用脉冲电镀工艺获得了高密度的纳米孪晶铜。为了进一步揭示孪晶形成的影响因素，研究了系列 MPS 浓度在镀液中的作用。当镀液中并未添加 MPS 时，镀层由粗大的晶粒组成，平均晶粒大小为 0.9 μm，晶粒内部含有少量的垂直或倾斜于膜面的孪晶界，镀层的晶粒取向为（110）和（111）共存，两者织构比例分别为 49%和 27.8%。从 FIB 微观组织观察和 X 射线衍射的结果可知，当镀液中添加 10 ppm 的 MPS 后，镀层组织变为柱状纳米孪晶铜组织，柱状晶内部含有高密度水平方向的孪晶界，同时晶粒取向变为高度择优的（111）。当 MPS 含量从 10 ppm 持续上升至 40 ppm，镀层组织和晶粒取向无明显变化。具体地，当镀液中添加 40 ppm 的 MPS 时，镀层晶粒大小为 0.6 μm，且镀层晶粒（110）和（111）的织构比例分别为 3.45%和 95.1%。这说明，可以通过 MPS 的含量调节提高纳米孪晶铜电镀液的填充能力，而纳米孪晶微观组织的形成并不受影响。基于上述结果，我们使用该电镀液配方及工艺进行了大马士革微盲孔的填充。结果表明，当 MPS 含量为 40 ppm 时，可以实现大马士革微盲孔的无孔填充。纳米孪晶铜电镀液填充能力的提升使得纳米孪晶铜在 IC 制造应用成为可能，很大程度上促进了下一代互连材料的发展。

关键词：脉冲电镀；纳米孪晶铜；盲孔填充，大马士革工艺